

INFLUENCE OF NONLINEAR STIFFNESS ON THE DYNAMICS OF A SLENDER ELASTIC BEAM UNDER TORSIONAL OSCILLATIONS

Marcos Silveira*¹, Bento R Pontes Jr¹, José M Balthazar^{1,2}

¹Department of Mechanical Engineering,
UNESP - São Paulo State University, Bauru, SP, Brazil, 17033-360
m.silveira@feb.unesp.br, brpontes@feb.unesp.br

²Department of Applied Mathematics and Computation, IGCE,
UNESP - São Paulo State University, Rio Claro, SP, Brazil, 13506-900
jmbaltha@gmail.com

Keywords: slender beams, nonlinear stiffness, torsional oscillations.

Abstract. *This study focuses on analysing the effects of nonlinear torsional stiffness on the dynamics of a slender elastic beam under torsional oscillations, which can be subject to helical buckling. The helical buckling of an elastic beam confined in a cylinder is relevant to many applications. Some examples include oil drilling, medical cateters and even the conformation and functioning of DNA molecules. A recent study showed that the formation of the helical configuration is a result of only the torsional load, confirming that there is a different path to helical buckling which is not related to the sinusoidal buckling, stressing the importance of the geometrical behaviour of the beam. A low dimensional model of an elastic beam under torsional oscillations is used to analyse its dynamical behaviour with different stiffness characteristics, which are present before and after the helical buckling. Hardening and softening characteristics are present, as the effects of torsion and bending are coupled. With the use of numerical algorithms applied to nonlinear dynamics, such as bifurcation diagrams and basins of attraction, it is shown that the nonlinear stiffness can shift the bifurcations and induce changes in the stability of the desirable and undesirable solutions. Therefore, the proper modelling of these stiffness nonlinearities seems to be important for a better understanding of the dynamical behaviour of such beams.*

1 INTRODUCTION

For many years there's been interest of the oil industry on the helical buckling of drill-strings inside their wells. This type of structure operates, in many cases, beyond its buckling loads, both axial and torsional. Two post-buckling configurations are known, and named sinusoidal and helical. Sinusoidal buckling may occur with only axial load when the beam is confined in a cylinder. The common trend inside the oil industry is to understand the helical buckling as a consequence of larger compression after the sinusoidal buckling [1, 2]. However, a different path to helical buckling exists which is the result of torsional loads. This helical buckling may occur with axial loads of compression or tension [3].

Silveira & Wiercigroch [4] used the rotating torsional pendulum, showing that they provide useful results for drill-strings under torsional vibrations with stick-slip. Basins of attraction were used to illustrate the coexistence of a stable stick-slip limit cycle, a fixed point and an unstable limit-cycle. Thompson et al. [5] made a theoretical study of deformations and stability of a beam in continuous contact with a cylinder. New solutions were presented for the advanced post-buckling stage with torsional loadings with axial tension or compression on its ends.

The focus of this work is to study the dynamical behaviour of an elastic beam confined in a cylinder and under helical buckling. The stiffness characteristics of the structure, resulting from the helical geometric configuration, is included in a lumped parameter system by means of a nonlinear torsion spring. With this approach, it is possible to include hardening and softening effects. The influence of the nonlinear stiffness characteristics was analysed, and parameter ranges in which undesired phenomena occur were identified.

2 LOW DIMENSIONAL TORSIONAL MODELS OF DRILL-STRING DYNAMICS

Low dimensional models are useful tools to study separately some of the main vibration modes of drill-strings. The most common are 1 or 2 degree-of-freedom lumped parameter models for axial vibrations, whirling [6] or torsional vibrations [7]. More elaborated models involving coupling of two or three modes also exist. For example, models for coupled axial and bending vibrations [8], coupled axial and torsional vibrations [9] and coupled bending and torsional vibrations [10] have been used.

Torsional vibration is an important vibration mode in drill-strings, and is the one related to the stick-slip phenomenon. The drill-string can be modelled as a rotating torsional pendulum. Although not being able to reproduce fully the complex dynamics of the drilling system, the model permits the study of the main characteristics of the stick-slip oscillations. The assumption that the drill-pipes behave as a torsional spring is valid for a high ratio of mass moment of inertia of the BHA relative to the drill-pipes [7].

2.1 Modelling stick-slip oscillations

The self-sustained oscillations characteristic of systems with dry friction, known as stick-slip oscillations, are commonly studied with the use of the block-on-belt system, depicted in Figure 1(a). The torsional pendulum, depicted in Figure 1(b), is an equivalent stick-slip oscillator for torsional systems. The source of energy of the system is the constant velocity of the top drive, and this energy is transmitted to the drill-bit at the bottom via the drill-pipes. If at a certain time the friction torque is capable of stopping the drill-bit, elastic energy starts accumulating in the drill-pipes. After some time, the spring torque may achieve a value greater than the maximum static friction torque, allowing the drill-bit to start sliding. The system may come to a state in which the friction torque is able to stop the drill-bit again. This repetitive transition

from sliding to sticking motion of the drill-bit is what gives these oscillations their name.

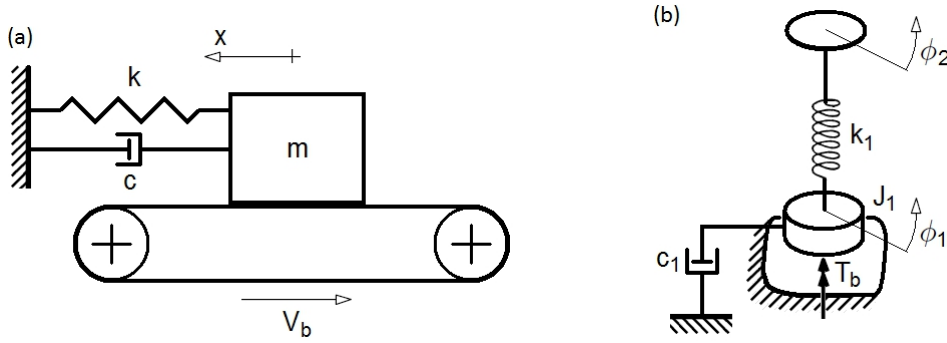


Figure 1: The classical block-on-belt system (a) and a 1-DOF rotating torsional pendulum with friction torque at the bottom (b) used to study torsional stick-slip oscillations

2.2 Rotating 1-DOF torsional pendulum system

As a first approximation, a drill-string can be modelled as a 1-DOF torsional pendulum. The equivalent inertia of the system is represented by a mass at the bottom, the drill-pipes are represented by a torsional spring, the equivalent damping acting on the system is represented by a torsional damper. Also as a first approximation, the angular velocity of the rotary table is considered as constant, as the amplitude of its oscillations is considerably smaller than the oscillations of the velocity of the bit [7]. The equation of motion for this system is:

$$J_1 \ddot{\phi}_1 + c_1 \dot{\phi}_1 + k_1 (\phi_1 - \phi_2) - T_b = 0, \quad (1)$$

in which J_1 is the equivalent mass moment of inertia of the drill-string, c_1 is the equivalent damping coefficient, k_1 is the equivalent linear torsional stiffness of the drill-pipes, ϕ_1 is the angular position of the drill-bit, ϕ_2 is the angular position of the rotary table at the top of the drill-string, T_b is the torque-on-bit and a dot denotes differentiation over time.

In this problem, the interest is in the relative displacement between the top and the bottom, as the torque stored in the spring, representing the drill-pipes, depends on this quantity. With this in mind, the relative angular displacement between the rotary table and the bit is defined as:

$$\phi = \phi_1 - \phi_2, \quad (2)$$

While investigating the behaviour of elastic beams confined in a cylinder, it was seen that these slender structures may experience helical buckling [5]. Because of this post-buckling behaviour, hardening or softening characteristic of the stiffness may arise due to coupling between torsion, bending and extension or compression of the beam, this effect being one of the sources of nonlinearities in the system. Based on that, in this work we incorporate this helical buckling geometrical behaviour into the low dimensional lumped parameter model. This is done by introducing a nonlinear term on the torsional stiffness characteristic of the drill-pipes.

The nonlinear stiffness potential and the resulting torque are given by:

$$V = \frac{k_1 \phi^2}{2} + \frac{k_2 \phi^4}{4} \quad \text{and} \quad T = k_1 \phi + k_2 \phi^3 \quad (3)$$

Both the elastic potential and the torque are shown in Figure 2 for values of k_2 representing linear ($k_2 = 0$, solid), hardening ($k_2 = 0.9$, dash) and softening springs ($k_2 = -0.2$, dash-dot). Introducing the nonlinear torque term on (1) results in the equation of motion of the nonlinear system:

$$J_1 \ddot{\phi}_1 + c_1 \dot{\phi}_1 + k_1 \phi + k_2 \phi^3 - T_b = 0 \quad (4)$$

In order to take into consideration the oscillations of the rotary table while the bit is experiencing stick-slip, which is observed in field data [7], it is possible to include the dynamics of the drive system, resulting in a 3-DOF electromechanical model.

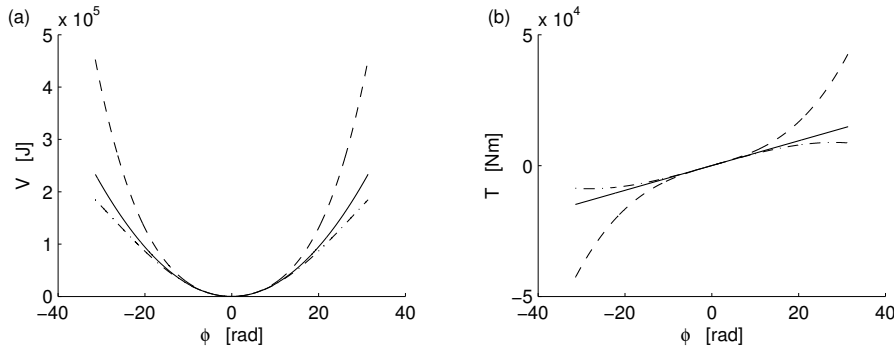


Figure 2: Elastic potential energy (a) and elastic torque (b) as function of ϕ for linear ($k_2 = 0$), hardening ($k_2 = 0.9$) and softening springs ($k_2 = -0.2$)

The simplest model for the torque-on-bit (T_b) is a piecewise Coulomb-like friction law, with a value for static friction ($T_{b,s}$) and a lower value for dynamic friction ($T_{b,d}$), which in this case is independent of the velocity $\dot{\phi}_1$. This model can be written as:

$$T_b = \begin{cases} T_{b,s} = \mu_s W_b & \text{if } \dot{\phi}_1 = 0 \\ T_{b,d} = \mu_d W_b & \text{if } \dot{\phi}_1 \neq 0 \end{cases}, \quad (5)$$

in which μ_s is the static coefficient of friction, μ_d is the dynamic coefficient of friction and W_b is the normal reaction at the bit (weight-on-bit or WOB). This model has discontinuities at the transition from negative to positive velocities and at the transition from static to dynamic friction, the cause of a discontinuity on the bifurcation diagram of stick-slip systems.

It is known that the friction torque has some dependency on the relative velocity. Also, the transition from the static to dynamic friction is not a discontinuous one, but a smooth transition. In order to include such properties, more elaborated models exist to describe the friction curve. A comprehensive survey of various friction models and their classification is given by Wojewoda *et al.* [11]. However, it was shown that the Coulomb model is a reasonable approximation for the torsional pendulum with stick-slip oscillations [4].

2.3 Coexisting attractors on the rotating torsional pendulum with stick-slip

This damped system with the Coulomb dry friction model is a non-smooth system [12], characterised by having a phase space consisting of two regions. Three qualitatively different phase space configurations are possible, depending on a combination of the velocity and the damping coefficient [13]. In one configuration, a limit cycle flattened at the bottom, called the

stick-slip limit cycle, and a point attractor in its interior coexist, representing two possible steady state responses of the system. In this configuration, there is an unstable limit cycle between the attractors. All trajectories starting outside the limit cycle reach this attractor. Some trajectories starting in a region inside the limit cycle also reach this attractor. Other trajectories starting in a region closer to the centre of the spiral reach the point attractor. In another configuration is possible in which only the point attractor exists. This corresponds to a steady state motion without stick-slip oscillations, a desired configuration for the system. The parameters most commonly tuned are the velocity and the damping coefficient.

The location of the fixed point is given with the help of Eq. (4), which will be valid for $\dot{\phi}_1 \geq 0$, above the sliding surface lies. It is the equation of a spiral, with the fixed point being the focus of this spiral, given by the solution of:

$$c_1 \dot{\phi}_1 + k_1 \phi + k_2 \phi^3 = T_{b,d} \quad (6)$$

To determine the location of the stick-slip limit cycle, it is possible to take as a starting point the stick-to-slip transition. Starting from there, the trajectory follows Eq. (1) until it reaches the sliding surface again. It then moves along the sliding surface until it returns to the stick-to-slip transition point, which is given by the solution of:

$$k_1 \phi + k_2 \phi^3 = T_{b,s}. \quad (7)$$

The division of the phase space is at $\dot{\phi}_1 = 0$, where the velocity and friction torque change sign. This division comes from the discontinuous characteristic of the friction torque used.

3 NUMERICAL RESULTS

The highly non-linear model, exhibiting relaxation vibrations, nonlinear stiffness and discontinuities because of the friction models, was investigated with numerical simulations, using a 4th order Runge-Kutta solver. The base parameters used in these results are $J_1 = 374 \text{ kgm}^2$, $c_1 = 42 \text{ Nms}$, $k_1 = 473 \text{ Nm}$, $\Omega_2 = 4.6 \text{ rad/s}$, $T_{b,d} = 4000 \text{ Nm}$ and $T_{b,s} = 2000 \text{ Nm}$.

Extensive work has been done in simulation of non-smooth systems, and specifically in systems undergoing stick-slip oscillations [13, 14, 15, 16]. The simulations of these non-smooth systems have to separate the non-smooth phase space into a series of adjacent smooth regions. In this case, two regions are necessary, one for the stick mode and one for the slip mode. A switch function is used to perform the transitions from stick to slip modes. This is done by monitoring the velocity and the torque built in the torsional spring to determine in which mode the system is, and selecting the equations of motion accordingly.

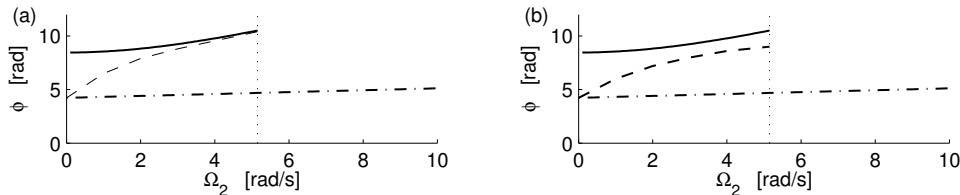


Figure 3: Bifurcation diagram for varying Ω_2 showing the switch from region with stick-slip to region without stick-slip. The solid line represents the stick-slip limit cycle, the dashed line represents the unstable limit cycle, and the dash-dot line represents the fixed point.

Bifurcation diagrams confirm that there is a region in parameter space corresponding to operation without stick-slip oscillations. For values of the motor velocity (Ω_2) less than $\Omega_2^* = 5.227$ rad/s, the system presents large amplitude stick-slip limit cycle, while for values of Ω_2 greater than Ω_2^* the system presents a fixed point (Figure 3). This region is related to a combination of high angular velocities of the rotary table and high damping coefficient of the drill-string.

3.1 Influence of systems parameters on the stability of the stick-slip limit cycle

A broad range of parameters is considered to analyse the fold bifurcation through which the stick-slip limit cycle is destroyed, including the inertia of drill-string (J_1), damping coefficient (c_1) and linear torsional stiffness (k_1). The influence of these variations were observed on the twist (ϕ) and bit speed ($\dot{\phi}_1$). The bifurcation diagrams are very similar to the ones in Figure 3, although only the stable stick-slip limit cycle (dashed line) and the point attractor (solid line) are shown. It is seen that the destruction mechanism of the limit cycle is maintained. Initially, the value of k_2 is set to zero, and an analysis of this parameter is performed later.

By varying the inertia of the drill-string, it is possible to see that the limit cycle does not exist for higher values of inertia. However, this can hardly be considered a control parameter. It can be seen that a typical drill-string of 2000 m of length has an equivalent inertia close to 380 kgm², which is very close to the bifurcation value for this parameter. The damping coefficient is one of the most important parameters to tune in order to try to eliminate stick-slip oscillations, together with the motor velocity. Usual values for this parameter lie in the range between 30 Nms and 60 Nms, and are shown here to be around the bifurcation value $c_1^* \approx 42.48$ Nms.

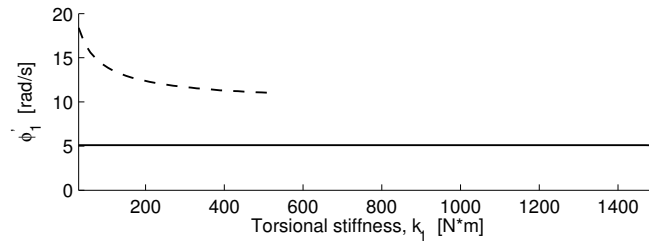


Figure 4: Bifurcation diagrams for bit velocity for the variation of the linear torsional stiffness

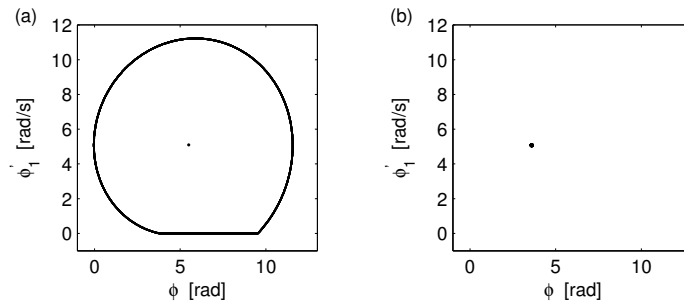


Figure 5: Phase planes at $k_1 = 405$ Nm (a), showing the coexisting fixed point and stick-slip limit cycle, and at $k_1 = 600$ Nm (b), showing the sole existing fixed point

The torsional stiffness is influenced mainly by the drill-pipe section. It is interesting to note that stick-slip is of higher concern as the linear torsional stiffness diminishes, demonstrating that

the problem has higher occurrence for longer and more slender drill-strings. From Figures 4 and 5 it is observed that the bifurcation value, $k_1^* \approx 510.84 \text{ Nm}$, is close to 470 Nm, the torsional stiffness of a typical drill-string with 2000 m.

Parameter plots can be generated to show the non-smooth fold bifurcation related to the disappearance of the stick-slip limit cycle as function of relevant parameters of the system. Two of these parameter plots, for c_1 and J_1 , and for k_1 and J_1 are shown in Figure 6, in which the lighter region corresponds to motion with stick-slip and the darker region corresponds to motion without stick-slip. In both plots, J_1 was varied from 0 to 2000 kgm^2 , and it is possible to see that the bifurcation values of c_1 and k_1 decrease for higher values of J_1 . Also, it is possible to see that the slope on Figure 6-b changes more abruptly close to $k_1 = 400 \text{ Nm}$.

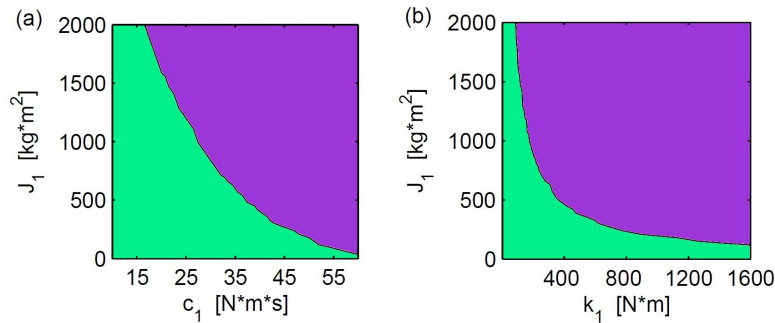


Figure 6: Parameter plots for c_1 and J_1 (a) and for k_1 and J_1 (b), showing the fold bifurcation related to the disappearance of the stick-slip limit cycle. The green region corresponds to motion with stick-slip and the purple region corresponds to motion without stick-slip

3.2 Nonlinear stiffness of drill-pipes as a result of helical buckling

The behaviour of the system with nonlinear torsional stiffness is comparable to the one with linear stiffness. The fixed point and the stick-slip limit cycle coexist for a large range of the parameters. However, the bifurcation point in which the stick-slip limit cycle ceases to exist is influenced by the value of the nonlinear stiffness coefficient k_2 , as seen in the bifurcations diagrams for varying Ω_2 (Figure 7). A softening spring tends to bring the bifurcation point to the left of the diagram, while a hardening spring tends to push this point to the right.

Figure 8 shows bifurcations diagrams for varying k_2 for two values of Ω_2 : 4 rad/s (a) and 6 rad/s (b). These results confirm what was observed from the system with linear stiffness, in which the increase in the angular velocity results in a larger range of parameters for operation without stick-slip occurrence. In these diagrams, this effect is observed as the bifurcation point moves to the right as Ω_2 increases.

Figure 9 shows three phase portraits relative to Figure 8(a). It is possible to observe that throughout the range of k_2 there is no qualitative change, and the results agree with the model with linear stiffness. Figure 10 shows equivalent phase portraits relative to Figure 8(b). For this larger velocity, the results with the softening ($k_2 = -0.2$) and linear ($k_2 = 0$) springs are similar, meaning the stick-slip limit cycle is not present. However, the result with the hardening spring ($k_2 = 0.9$) shows that the limit cycle is still present at this value of Ω_2 , which is larger than the bifurcation point seen with the linear spring. This result stresses the importance of taking into account the nonlinear torsional characteristics of the structure.

Taking the bifurcation point for Ω_2 at $k_2 = 0$, a continuation was performed to locate this fold

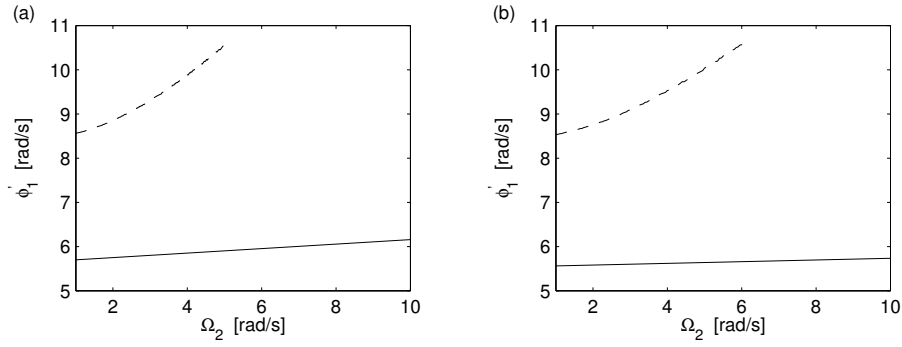


Figure 7: Bifurcation diagrams for varying Ω_2 for a softening spring with $k_2 = -0.2$ (a) and a hardening spring with $k_2 = 0.9$ (b), showing the fold by which the stick-slip limit cycle ceases to exist. The solid line represents the fixed point, while the dashed line represents the stick-slip limit cycle

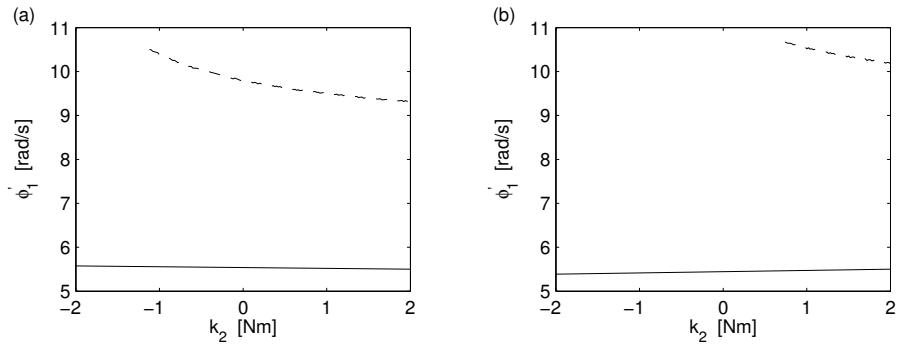


Figure 8: Bifurcation diagrams for varying k_2 for two values of Ω_2 : 4 rad/s (a) and 6 rad/s (b). The solid line represents the fixed point, while the dashed line represents the stick-slip limit cycle

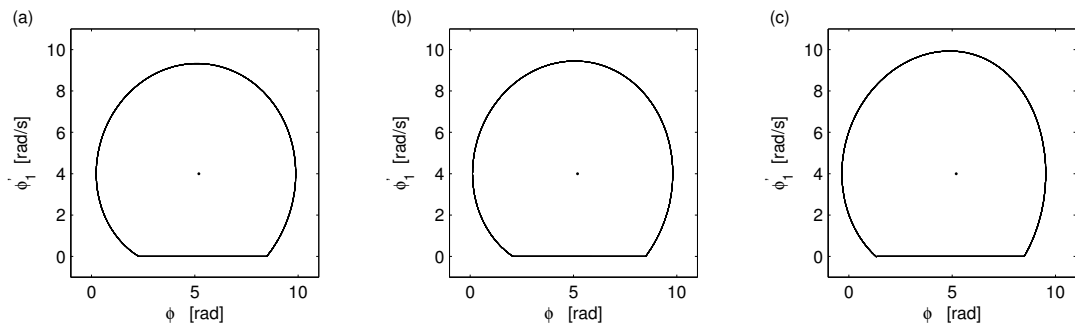


Figure 9: Phase portraits with $\Omega_2 = 4$ rad/s at three values of the nonlinear stiffness coefficient: $k_2 = -0.2$ (a), $k_2 = 0$ (b) and $k_2 = 0.9$ (c), showing the stick-slip limit cycle and fixed point

bifurcation as k_2 varies. The results are shown in Figure 11, which indicates that the bifurcation exists for a significant range of the nonlinear stiffness coefficient.

4 CONCLUSIONS

The rotational torsional pendulum has shown to be effective in studying many aspects of torsional vibrations in isolation. In this work a lumped parameter model was developed which

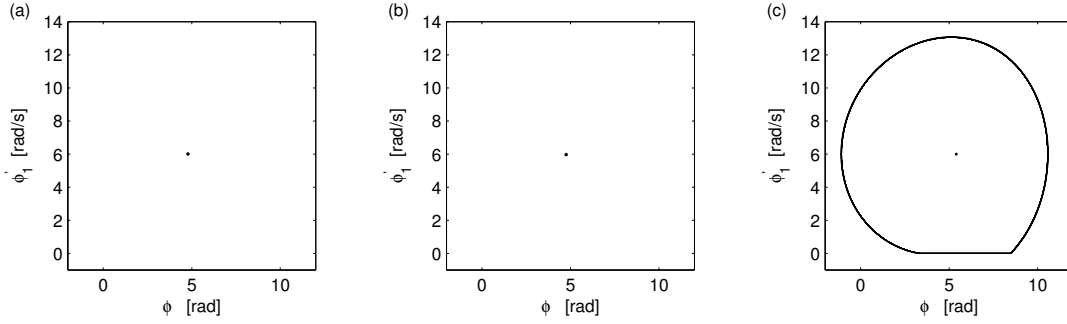


Figure 10: Phase portraits with $\Omega_2 = 6$ rad/s at three values of the nonlinear stiffness coefficient: $k_2 = -0.2$ (a), $k_2 = 0$ (b) and $k_2 = 0.9$ (c), showing stick-slip limit cycle and fixed point

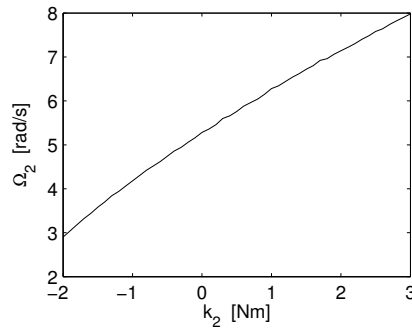


Figure 11: Position of the fold bifurcation related to the disappearance of the stick-slip limit cycle as function of k_2 and Ω_2 . The region above the line indicates operation without stick-slip occurrence

incorporates the helical buckling geometrical behaviour, which was done by introducing a nonlinear term on the torsional stiffness characteristic of the drill-pipes.

Bifurcation diagrams allowed to find Ω_2^* above which the system operates without stick-slip oscillations. A combination of angular velocities and damping on the system can also avoid stick-slip oscillations. Apart from these two parameters, the system was also observed under variation of a broad range of parameters. The same bifurcation scenario repeats for almost all parameters, which suggests that operational conditions such as drill-bit–rock combination should also be taken into consideration when searching for stick-slip free parameters. Typical parameters for a drill-string of 2000 m are close to the bifurcation values, and as the length of the drill-string increases, the inertia and torsional stiffness can determine occurrence or not of stick-slip.

The results using the hardening spring shows that the limit cycle is still present at larger values of Ω_2 , compared to the bifurcation point seen with the linear spring. Also, the bifurcation exists for a significant range of the nonlinear stiffness coefficient. These results stress the importance of taking into account the nonlinear torsional characteristics of the structure.

An experimental rig is being used to determine the exact expression of the nonlinear elastic torque, and the results will improve the accuracy of the low dimensional model.

5 ACKNOWLEDGEMENTS

The authors thank the Brazilian funding agencies FAPESP (project #2012/19774-3), CNPq and CAPES.

REFERENCES

- [1] A. Lubinski, W.S. Althouse, J.L. Logan, Helical buckling of tubing sealed in packers, *Petroleum Transactions*, 1962, 655–670.
- [2] N.C. Huang, P.D. Pattillo, Helical buckling of a tube in an inclined wellbore, *International Journal of Non-Linear Mechanics*, **35**, 2000, 911–923.
- [3] G.H.M. Heijden, The static deformation of a twisted elastic rod constrained to lie on a cylinder, *Proceedings of the Royal Society A*, **457**, 2001, 695–715.
- [4] M. Silveira, M. Wiercigroch, Low dimensional models for stick-slip vibration of drill-strings, *Journal of Physics: Conference Series*, **181**, 2009.
- [5] J.M.T. Thompson, M. Silveira, G.H.M. Heijden, M. Wiercigroch, Helical post-buckling of a rod in a cylinder: with applications to drill-strings, *Proc. R. Soc. Lond. A*, **468**, 1591–1614, 2012.
- [6] A.P. Christoforou, A.S. Yigit, Dynamic modelling of rotating drillstrings with borehole interactions, *Journal of Sound and Vibration*, **206**, 243–260, 1997.
- [7] J.D. Jansen, L. Steen, L., Active damping of self-excited torsional vibrations in oil well drillstrings, *Journal of Sound and Vibration*, **179**, 257–279, 1995.
- [8] A.S. Yigit, A.P. Christoforou, Coupled axial and transverse vibrations of oilwell drilltrings, *Journal of Sound and Vibration*, **195**, 617–627, 1996.
- [9] T. Richard, C. Germy, E. Detournay, A simplified model to explore the root cause of stick-slip vibrations in drilling systems with drag bits, *Journal of Sound and Vibration*, **305**, 432–456, 2007.
- [10] A.S. Yigit, A.P. Christoforou, Coupled torsional and bending vibrations of drilltrings subject to impact with friction, *Journal of Sound and Vibration*, **215**, 167–181, 1998.
- [11] J. Wojewoda, A. Stefanski, M. Wiercigroch, T. Kapitaniak, T., Hysteretic effects of dry friction: modelling and experimental studies, *Philosophical Transactions of the Royal Society A*, **366**, 747–765, 2008.
- [12] M. Bernardo, C.J. Budd, A.R. Champneys, P. Kowalczyk, *Piecewise-smooth dynamical systems*, Springer–Verlag, London, 2008.
- [13] U. Galvanetto, U., Sliding bifurcations in the dynamics of mechanical systems with dry friction – remarks for engineers and applied scientists, *Journal of Sound and Vibration*, **276**, 121–139, 2004.
- [14] K. Popp, M. Rudolph, Vibration control to avoid stick-slip motion, *Journal of Vibration and Control*, **10**, 1585–1600, 2004.
- [15] M. Wiercigroch, A note on the switch function for the stick-slip phenomenon, *Journal of Sound and Vibration*, **175**, 700–704, 1994.
- [16] R.I. Leine, D.H. Campen, D. H., Bifurcation phenomena in non-smooth dynamical systems, *European Journal of Mechanics A/Solids*, **25**, 596–616, 2006.